Optical characterization of charge transfer and bonding dimer plasmons in linked interparticle gaps

2011 New J. Phys. 13 083013

(http://iopscience.iop.org/1367-2630/13/8/083013)

New Journal of Physics
The open-access journal for physics

Optical characterization of charge transfer and bonding dimer plasmons in linked interparticle gaps

O Pérez-González[1,2], N Zabala[1,2] and J Aizpurua[2,3]

[1] Department of Electricity and Electronics, University of the Basque Country UPV/EHU, 48080 Bilbao, Spain
[2] Donostia International Physics Center (DIPC) and Centro de Física de Materiales, Centro Mixto CSIC-UPV/EHU, Paseo Manuel Lardizabal 4, 20018 Donostia/San Sebastián, Spain
E-mail: aizpurua@ehu.es

New Journal of Physics **13** (2011) 083013 (16pp)
Received 31 May 2011
Published 12 August 2011
Online at http://www.njp.org/
doi:10.1088/1367-2630/13/8/083013

Abstract. We present a theoretical study of the optical properties of nanoparticle dimers connected by conductive gap linkers. The geometrical and conductive properties of the linker modify strongly the optical response of the linked metallic cavity. Two plasmonic modes are responsible for the main spectral features of the cavity: a bonding dimer plasmon (BDP) and a charge transfer plasmon (CTP). We first explore how these two modes are modified as a function of the geometry and the conductance through the cavity, identifying the spatial distribution of the linking current densities. Furthermore, we introduce a resonant feature in the conductivity of the linker, where we observe a complex splitting of the plasmon modes. We also study the capabilities of the BDP and CTP modes in localized surface plasmon resonance (LSPR) sensing.

[3] Author to whom any correspondence should be addressed.

Contents

1. Introduction

The interaction between electromagnetic waves and plasmonic nanostructures has become an important field of research in nanophotonics. In the last decade, there have been significant advances in plasmonics [1, 2], resulting in a better understanding of the optical properties of a variety of metallic nanostructures with extensive applications in spectroscopy, biomedicine, etc, where plasmons localize and enhance the fields [3–8]. When two nanoparticles are placed next to each other, they no longer behave individually, but as a new interacting system where the plasmon modes of the individual nanoparticles interact and result in hybridized dimer plasmon modes [9–11]. In particular, the dipolar bonding dimer plasmon (BDP), with strongly localized charge densities of opposite sign and enormously enhanced local electromagnetic fields in the dimer cavity, has been deeply studied due to its potential applications in surface enhanced Raman scattering (SERS) [12–15]. When two nanoparticles are closely located establishing a conductive overlap between them, a charge transfer plasmon (CTP) mode, which allows current density through the cavity, emerges, involving an oscillating distribution of net charge at every individual nanoparticle [16–23].

In parallel with the development of plasmonic cavities, electronic transport through molecules has become a vibrant field in nanoscience due to its potential technological applications in nanoelectronics, connected to novel nanofabrication and nanomanipulation methods and improved current detection schemes [24–32]. In recent years, there has been growing interest in the interaction between the plasmonic modes and molecular excitations, since the control of the coupling of molecular complexes to metallic structures is very important for the development of active plasmonics components dealing with optoelectronic signals [33–36]. Among the broad range of potential applications of these systems we can find light harvesting structures, molecular switches or modulators. In particular, it has been shown that in systems composed of metal nanoparticle–molecular complexes, the presence of molecules shifts the plasmon mode by changing the interaction between the molecular and plasmonic resonances [37, 38].

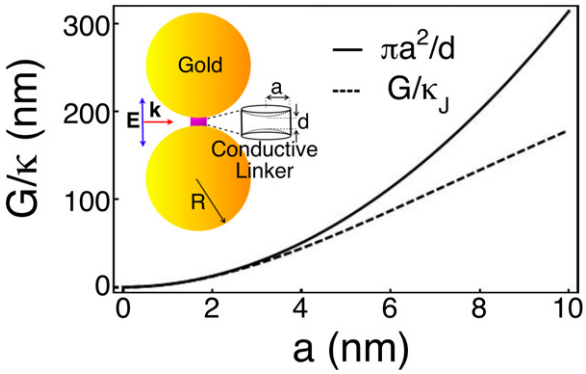

Figure 1. Ratio conductance/conductivity for a perfect conductive cylinder with planar endings, where $G/\kappa = \pi a^2/d$ (solid line), and for a conductive linker with curved endings, where G/κ is given by equation (2) (dashed line). The inset is a schematic representation of a gold dimer connected by a linker. The linker is zoomed so that its concave endings and geometrical parameters, radius a and length d, can be clearly appreciated ($d = 1$ nm, $R = 55$ nm).

To account for the merge of plasmonics and electronics, we presented in a recent letter the connection between the optical properties of the BDP and CTP and the transport properties of the metallic cavity [39]. Here, we extend our previous results by considering strong modifications in the geometry of the junction (solid block versus ring-like linker), as well as by introducing spectral resonant behaviour in the conductivity and analysing its effect in the optical spectrum. Finally, we also study the potential of the system for localized surface plasmon resonance (LSPR) sensing applications based on spectral shifts.

In order to analyse the optical response of the system, we solve Maxwell's equations in the presence of inhomogeneous media using the boundary element method (BEM) to obtain the electromagnetic fields and the optical extinction spectrum [40, 41].

2. Bonding dimer plasmon versus charge transfer plasmon in conductive junctions

2.1. Optical response of the conductive junction

The shape and size of the constituents are two key ingredients in the study of plasmonic systems. We therefore define the geometry of our system in the schematics included in figure 1. We consider a heterogeneous nanostructure composed of two nanoshells, acting as electrodes, with silica cores of radius $R_{\text{int}} = 45$ nm; covered with a gold shell of radius $R = 55$ nm, namely, the thickness of the gold shells is 10 nm. The conductive linker connecting the dimer is modelled as a solid cylinder perfectly matching the spherical shape of the electrodes. The linker is characterized by two parameters: the radius a and the length d, which is the shortest interparticle distance between the nanoshells. In our study we consider the interparticle distance to be $d = 1$ nm, so that the nanoshells are strongly coupled. The incident light is a plane wave with linear polarization along the symmetry axis of the system and wave vector $\mathbf{k}$ perpendicular to the same symmetry axis.

The surrounding medium is another key feature influencing the plasmonic properties. In our case, the dimer is assumed to be suspended in vacuum and the materials composing the

different parts of the system are characterized by local dielectric functions, $\varepsilon(\omega)$, taken from the literature, both for gold [42] and silica [43]. For the sake of simplicity, we have first modelled the conductive junction as a pure conductor characterized by a dc conductivity κ_J, so that its frequency-dependent dielectric function can be expressed as

$$\varepsilon(\omega) = 1 + \mathrm{i}\frac{4\pi\kappa_J}{\omega}. \tag{1}$$

The conductivity of the junction κ_J is then related to its conductance G through geometric parameters. In our case, the consideration of the spherical connection between the linker and the particles leads to a mathematical expression for the ratio G/κ_J involving the parameters a, R and d:

$$\frac{G}{\kappa_J} = \frac{G}{\kappa_J}(a, R, d) = \pi\left\{\sqrt{R^2 - a^2} - R + (d/2 + R)\ln\left[1 + 2(R - \sqrt{R^2 - a^2})/d\right]\right\}, \tag{2}$$

where R is the external radius of the nanoshell, a is the radius of the junction and d is the interparticle distance. In the limit of very thin junctions, $a \ll d$, the function $G/\kappa_J(a, R, d)$ (see equation (2)) behaves as the relation for a conductive cylindrical wire with planar endings, as expected:

$$\lim_{a \ll d, R} \frac{G}{\kappa_J} = \frac{\pi a^2}{d}. \tag{3}$$

We note that the real part of $\varepsilon(\omega)$ is frequency independent (see equation (1)), since we had assumed the junction to be a pure conductor. In contrast, the imaginary contribution, which is related to energy losses, is the only part of the dielectric function affected by any possible change in the parameters. These changes in the imaginary part of $\varepsilon(\omega)$ can be related to the variation of dc conductivity κ_J, which is governed by variations in the geometry, variations in the conductance or a combination of both. Whereas in the limit of very thin junctions the conductance has a quadratic dependence on the radius of the junction, as shown in equation (3), a nearly linear trend is obtained in equation (1) when thicker junctions are considered. We can observe in figure 1 that this means that G/κ_J is below the parabola given by the function of a wire, due to the effect of the curvature of the nanoshells. For the interparticle distance considered in the present work, $d = 1$ nm, this implies quadratic behaviour of G/κ_J up to radius $a \simeq 3$ nm, as appreciated in figure 1. In order to connect with the terminology for molecular conductances, we will vary κ_J so that the total conductance of the molecule is equal to an integer number n of quantum units of conductance G_0, i.e. $G = nG_0$, where $G_0 = 2e^2/h \approx 77.5\,\mu$S. In section 3, we will consider a more general dielectric response using a Drude–Lorentz model to characterize the existence of an exciton in the optical response of the linker, and we will have the opportunity to explore the differences between both situations.

2.2. Spectral behaviour of bonding dimer plasmon and charge transfer plasmon modes

We analyse a gold nanoshell dimer linked by a conductive junction as the conductance of the junction is varied, finding two main trends: the BDP mode associated with low values of conductance and the CTP mode in the large conductance regime [39]. As we have already mentioned, the aim of this study is to find a connection between plasmonics and nanoelectronics and, to this end, we first study the optical behaviour of the system when the conductance G through the junction is varied while the size of the linker is fixed. For instance, this situation

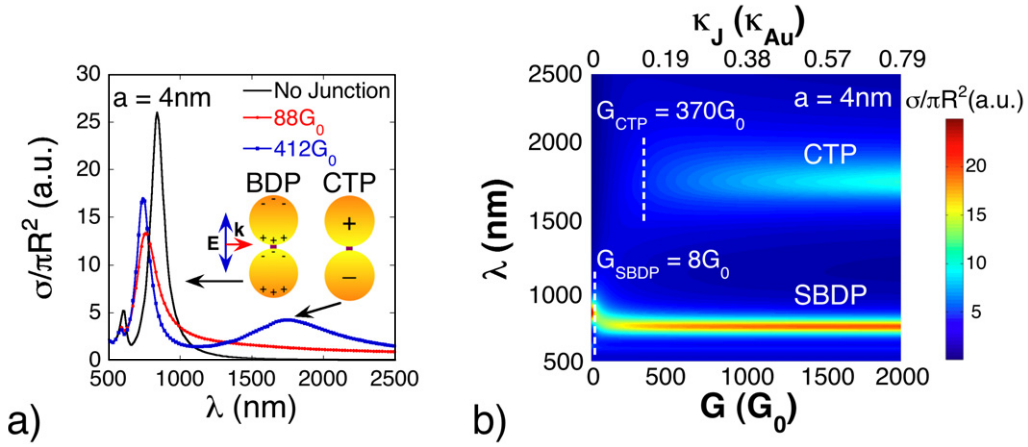

Figure 2. (a) Calculated normalized optical extinction cross-section for a gold nanoshell dimer with and without a conductive linker of radius $a = 4\,\text{nm}$. We consider two cases with a linker: one with low conductance showing a blue-shift and broadening of the BDP mode and the other with high conductance showing the emergence of the CTP mode. (b) Colour map of the calculated normalized optical extinction cross-section, showing the evolution of the plasmonic resonances, SBDP and CTP, in a gold nanoshell dimer with interparticle distance $d = 1\,\text{nm}$, linked by a conductive junction with radius $a = 4\,\text{nm}$ as the conductance G and thus the conductivity κ_J are increased for different wavelengths λ. The threshold values of conductance G_{SBDP} and G_{CTP} were obtained from equations (4) and (5), respectively.

corresponds to a system where we change the nature of the junction but the geometry remains unaltered. For the case of the BDP, we find that this mode is blue-shifted and its intensity decreases as G is increased, forming a screened BDP mode (SBDP), where the electric field is progressively expelled from the junction. In the case of the CTP mode, we find that, in contrast to the BDP, higher values of conductance G are needed for the CTP to emerge. Figure 2(a) shows a comparison of the calculated normalized optical extinction cross-section for a gold nanoshell dimer with and without a linker. When there is no junction, we observe the BDP mode at $\lambda = 840\,\text{nm}$, which can be understood in terms of the hybridization of the dipolar modes ($l = 1$) of every individual nanoshell resulting in a dipole–dipole interaction [9] (see the schematics included in figure 2(a)). A bonding mode coming from the hybridization of the quadrupolar modes ($l = 2$) of the individual nanoparticles can also be observed as a small feature around $\lambda \approx 600\,\text{nm}$. In contrast, when we consider a junction with a conductance of about $88G_0$, the BDP loses intensity, broadens and is blue-shifted as a consequence of the screening of the interaction at the cavity forming an SBDP. The quadrupolar mode also loses strength as the conductance increases. For large conductance values of $412G_0$, the SBDP mode partially recovers its intensity and a CTP mode emerges at $\lambda = 1750\,\text{nm}$ from the coupling of the monopolar ($l = 0$) individual nanoshell modes, resulting in a dipolar pattern involving both particles. This mode implies a net charge transfer between both nanoshells (see the schematics included in figure 2(a)).

To establish the connection between the electronic transport and optical processes [39], we relate the time of the optical cycle t_{op}, associated with both plasmon resonances ω_{BDP} and

ω_{CTP}, to the transport time t_{e} of the electrons through the cavity related to the conductivity. Based on this connection, it is possible to obtain mathematical expressions for the conductance thresholds, G_{SBDP} and G_{CTP}, where the BDP mode becomes the SBDP mode and the CTP emerges, respectively [39]. Explicitly, the expression providing the conductance threshold for the modification of the BDP into a screened SBDP mode is

$$G_{\mathrm{SBDP}} = \frac{\omega_{\mathrm{BDP}}}{2\pi}\frac{a^2}{d}, \tag{4}$$

whereas the conductance threshold for the CTP to appear is

$$G_{\mathrm{CTP}} = \frac{\omega_{\mathrm{CTP}}}{4\pi}\frac{R^2}{d}. \tag{5}$$

While equation (4) indicates that the SBDP mode has a strong dependence on the geometry of the junction, i.e. on its conductivity, equation (5) shows that the CTP mode is related to the conductance of the junction rather than its conductivity, requiring larger conductance values than the SBDP ($R^2/2d > a^2/d$).

The evolution of these two modes is observed in figure 2(b), where we display a colour map of the calculated normalized optical extinction cross-section for a gold nanoshell dimer linked by a conductive junction with radius $a = 4$ nm as the conductance G and the conductivity κ_{J} are varied. We can see in detail how the BDP starts losing intensity and blue-shifts as G is increased, progressively turning into the SBDP. Then, the blue-shift reaches a saturation point from which the position of the resonance at $\lambda = 740$ nm remains unaltered despite the increase in conductance, and the mode gains intensity again as G is increased. Quantitatively, equation (4) predicts that conductance needs to reach values above $8G_0$ to form the SBDP in this situation, an estimation that is in good agreement with our simulations.

We can also observe the progressive emergence of the CTP at $\lambda = 1750$ nm in the near-infrared (NIR) part of the spectrum, occurring for large values of the conductance. Equation (5) predicts a threshold of $370G_0$, a value that is consistent with our calculations, as observed in figure 2(b). It should be noted that the SBDP recovers spectral weight, in parallel with the emergence of the CTP, once the spectral position of the SBDP becomes constant. Thus, we can understand the relative weight of the resonances in terms of the increase in conductivity, which leads to a modification of the dielectric function. Note also that the increase of conductance while the radius of the junction is fixed implies that the number of electrons contributing to the electric current density is also increased.

So far, we have only considered the variation of conductance through the junction while its size remains unaltered. We now maintain the conductivity fixed while the radius of the linker is varied, which corresponds to a physical situation where the material linking the nanoparticles is maintained while the size is varied, thus producing the variation of the linker's conductance G as well. Figure 3 shows the colour maps of the calculated normalized optical extinction cross-section to observe the evolution of the plasmonic resonances in a linked gold nanoparticle dimer with interparticle gap $d = 1$ nm, where the conductivity κ_{J} of the linkers is fixed whereas its radius a is varied. We observe that, under these conditions, the behaviour of both the BDP and the CTP modes differs from that previously. For the BDP, it is still possible to observe the blue-shift of the resonance, but its intensity decreases as the junction becomes wider (without regaining intensity). In the case of the CTP (in the top part of the maps, for longer wavelength values), after the emergence of the resonance we observe a considerable blue-shift as the

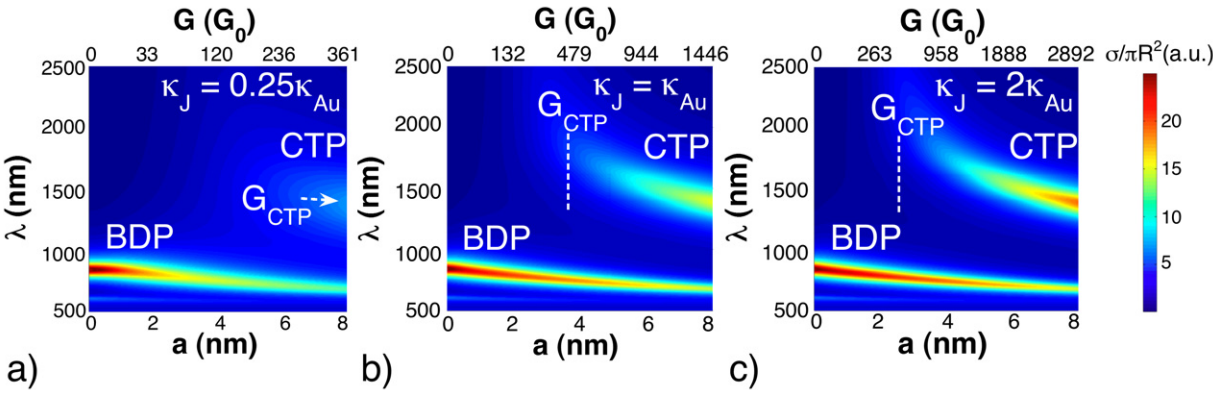

Figure 3. Colour maps of the calculated normalized optical extinction cross-section, showing the evolution of the plasmonic resonances BDP and CTP in a gold nanoparticle dimer with interparticle gap $d = 1$ nm linked by conductive molecular junctions, while the radius a is varied and conductivity κ_J is fixed: (a) $\kappa_J = 0.25\kappa_{Au}$, (b) $\kappa_J = 1.09\kappa_{Au}$ and (c) $\kappa_J = 2\kappa_{Au}$.

radius a is increased. However, in contrast to the BDP, this resonance becomes more intense as the junction becomes wider. We also notice that, while the BDP is present for any considered value of the conductance and radius, the CTP dies out for situations of low conductance and small radius. Similar behaviour has been previously reported in the literature for touching nanoparticle dimers and loaded antennas. Whereas for the touching nanoparticle dimers the optical response was governed by the interparticle distance [17], when considering loaded antennas, the size of the load and the free-carrier density at the cavity are the key ingredients controlling the optical response [21, 46]. In particular, these cases correspond to the colour map of figure 3(b), where the conductivity κ_J of the junction would be equal to the conductivity κ_{Au} of the gold shells acting as electrodes. We can also understand this behaviour in terms of the excitation of the BDP and CTP modes. The BDP mode, arising from the hybridization of the dipolar terms of the individual particles (see schematics in figure 2(a)), can exist for any value of the radius of the linker, losing intensity as the junction becomes wider and wider due to the increase in conductance. In contrast, the CTP mode, arising from the excitation of the monopolar ($l = 0$) individual nanoshell modes (see schematics in figure 2(a)), is not sustained, neither when there is no physical connection between the particles nor when the conductance is below G_{CTP}. This mode becomes the prominent resonant mode when conductance is large enough, satisfying the ordinary sum rules for the mode's excitation. Figure 3 also shows the threshold value, $G_{CTP} = 468G_0$, obtained from equation (5) (an arrow in figure 3(a) since the G_{CTP} falls outside the limits of the graphics). In this case, the threshold value, calculated for the saturated wavelength of the CTP, around $\lambda = 1390$ nm, points out that the higher the conductivity κ_J we consider for the junction, the narrower the junctions that can sustain the CTP resonance. This relation between the size and conductance of the junction and its conductivity was expected from equation (2), which also shows that when we increase the conductivity of the material, the amount of material needed to sustain conductance is reduced. Thus, these results could help us to establish a connection between the spectral changes in optical measurements and molecular conductance and/or size of molecular bridges.

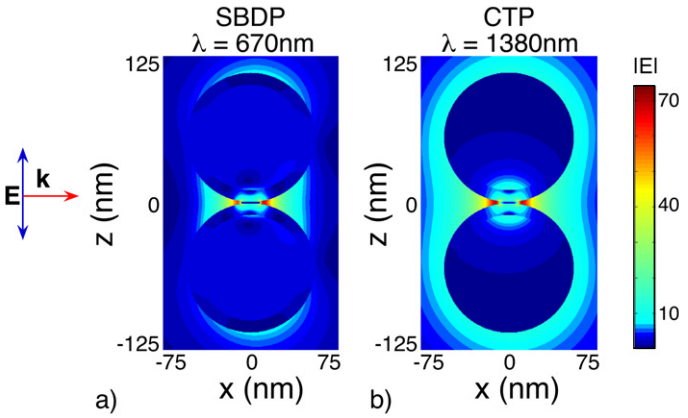

Figure 4. Near-field distribution of the SBDP and CTP modes for a nanoshell dimer linked by a conductive junction with radius $a = 8$ nm, conductivity $\kappa_J = 5\kappa_{Au}$ and conductance $G = 7229G_0$. (a) BDP corresponding to $\lambda = 670$ nm and (b) CTP corresponding to $\lambda = 1380$ nm.

2.3. Near-field distribution in the screened bonding dimer plasmon and charge transfer plasmon modes

The nature of the plasmon modes can be understood in an intuitive way by observing the near-field associated with the resonances. For the nanoparticle dimer linked by a conductive junction, the electric field is progressively expelled from the junction as the conductance is increased [39]. For low conductance values the junction still acts as a perfect capacitive cavity, whereas for values larger than the threshold value G_{SBDP} the local field is progressively expelled from the junction, reducing both the Coulomb attraction between the gold shells and the capacitance of the cavity.

This situation can be clearly observed in figure 4, where the modulus of the near-field is represented in the plane defined by the propagating vector **k** of the incident plane wave and the axis of polarization of the electric field **E** (see schematics in figure 4). To observe the different charge distributions of the SBDP and CTP resonances, we compare the near-field distributions of these two modes in figure 4, corresponding to a conductive junction with radius $a = 8$ nm and conductance $G = 7229G_0$: figure 4(a) corresponds to the SBDP resonance at $\lambda = 670$ nm and figure 4(b) corresponds to the CTP resonance at $\lambda = 1380$ nm.

In both cases, the local field is expelled from the junction and the near field takes its highest values around the molecular junction, but some differences can be observed. For the SBDP mode, the distribution of the field corresponds to a dipole–dipole pattern, as in the near-field distribution of the BDP distribution. In this case, the electric charge is highly localized at the cavity on every nanoparticle, with charge of opposite sign at both sides of the cavity, observing dipolar electric field distributions and fulfilling charge neutrality in every nanoparticle. In contrast, for the CTP mode, the near-field distribution has quite a uniform intensity distribution all around the dimer (see figure 4(b)), in agreement with the near-field patterns obtained by Romero *et al* [17]. In this case, the principle of charge neutrality in every nanoparticle is no longer valid and the whole nanostructure acts as a dipole. Another important feature of the CTP mode is the considerable penetration of the electric field inside the nanoparticles through the conductive junction. The parameter describing this ability of the electromagnetic

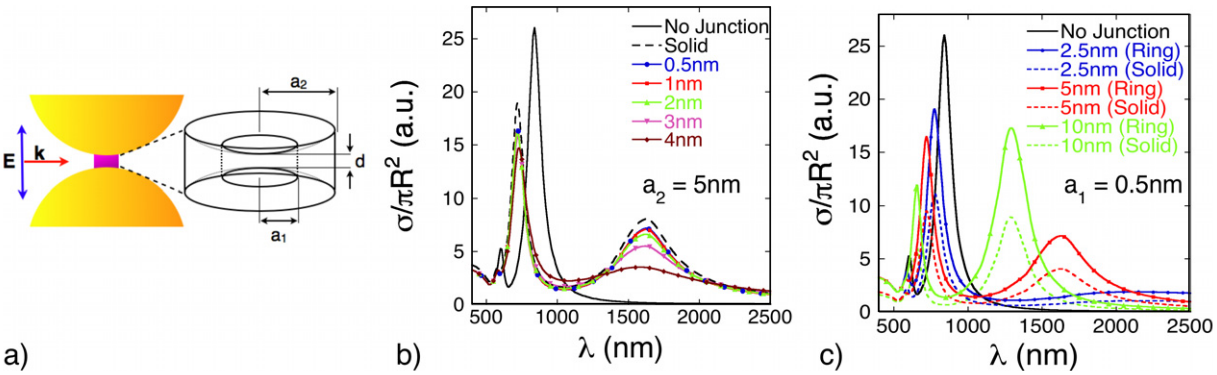

Figure 5. (a) Schematic representation of a gold nanoshell dimer linked by a hollow conductive junction having a ring-like shape. The junction is amplified so that its concave endings and its geometrical parameters, internal radius a_1, external radius a_2 and length d, can be clearly appreciated. (b) Calculated normalized optical extinction cross-sections for a nanoshell dimer linked by a cylindrical shell junction as the internal radius is varied from $a_1 = 0.5$ nm to $a_1 = 4$ nm. The external radius is $a_2 = 5$ nm and the conductivity is $\kappa_J = \kappa_{Au}$. The dashed line represents the spectrum corresponding to a dimer connected by a solid junction with radius $a = 5$ nm. Nanoshell parameters are $R_{int} = 45$ nm and $R = 55$ nm. (c) Calculated normalized optical extinction cross-sections for a nanoshell dimer linked by a conductive ring-like junction as the external radius is varied from $a_2 = 2.5$ nm to $a_2 = 10$ nm (solid lines). The internal radius is fixed at $a_1 = 0.5$ nm and the conductivity is $\kappa_J = \kappa_{Au}$. Dashed lines indicate the cases with solid junctions of the same external radii and the parameters for the nanoshells are the same as those in (b).

field to penetrate into a material is the skin depth δ, given in SI units by $\delta = \sqrt{2/\mu_0\omega\kappa}$ [44]. If we analyse the skin depth for the cases considered in figure 4, where $\kappa = \kappa_J = 5\kappa_{Au}$ and its corresponding conductance $G = 7229G_0$, we obtain values of $\delta_{SBDP}(\lambda = 670\,\text{nm}) \approx 12$ nm for the SBDP mode and $\delta_{CTP}(\lambda = 1625\,\text{nm}) \approx 17$ nm for the CTP mode. In most situations, such as those considered in this work, the conductance at the junction is much smaller; thus the skin depth is usually even larger. These values of the skin depth are either of the same order as the dimensions of the nanometric junction or much larger; therefore they allow for field penetration in most cases. For all the above, one can conclude that it is the intrinsic nature of the behaviour of conductance for the BDP and CTP modes that is the key aspect determining the spectral features of the system, rather than the skin depth [39].

2.4. Distribution of the electric current within the linker

In order to explore the properties of the currents through the junction, we study in this section how the optical response of the dimer is affected by morphological changes in the conductive junction. To that end, instead of a solid cylinder, we consider a hollow cylindrical shell, as depicted in figure 5(a). As for the solid case, the junction is characterized by its length d, corresponding to the interparticle gap. The junction is characterized by two parameters in this case: the internal and external radii of the conductive junctions a_1 and a_2, respectively. To study how these two parameters affect the optical response we explore different situations. For

example, if the external radius a_2 is fixed, we can vary the internal radius a_1, or vice versa, varying the amount of material holding the current density.

In the case of a ring-like junction, conductance and conductivity are related to each other via the geometric parameters

$$\frac{G}{\kappa_J}(a_1, a_2, R, d) = \pi \left\{ \sqrt{R^2 - a_2^2} - \sqrt{R^2 - a_1^2} + (R + d/2) \ln \left[\frac{(R + d/2) - \sqrt{R^2 - a_2^2}}{(R + d/2) - \sqrt{R^2 - a_1^2}} \right] \right\}, \tag{6}$$

which now involve the internal and external radii of the ring junction a_1 and a_2. It is quite clear from equation (6) that equation (2) is recovered in the limit $a_1 \to 0$, a situation where there is no hollow cavity in the junction. Thus, in this case, the conductivity of the ring-like junction is given by

$$\kappa_J = nG_0 \left\{ \pi \left\{ \sqrt{R^2 - a_2^2} - \sqrt{R^2 - a_1^2} + (R + d/2) \ln \left[\frac{(R + d/2) - \sqrt{R^2 - a_2^2}}{(R + d/2) - \sqrt{R^2 - a_1^2}} \right] \right\} \right\}^{-1}. \tag{7}$$

In figure 5(b), we represent the calculated normalized optical extinction cross-section for a gold nanoshell dimer linked by a conductive ring-like junction as the internal radius a_1 is increased while the external radius and conductivity are fixed to $a_2 = 5\,\text{nm}$ and $\kappa_J = \kappa_{Au}$, respectively. This situation creates an increasingly thinner ring sustaining smaller conductance. The results are compared to the case of a solid molecular junction with the same radius and the same conductivity. For small values of a_1, even though we remove the central part of the cylinder, the spectrum of the solid junction does not vary noticeably. This behaviour suggests that conduction through the molecular junction takes place mainly in the external region of the junction. This distribution of the current explains why the results of a solid junction are still reproduced when we remove wide central parts of the junction. In this case, the BDP mode red-shifts negligibly as the conductance decreases when considering thinner rings (with larger a_1), consistent with the behaviour of the BDP in solid junctions shown in figure 3. The spectral position of the CTP, when fully formed (once the conductance value allows for its appearance), remains at the same spectral position for a fixed external radius as the conductance is increased (decrease of a_1), consistent with the behaviour shown for the CTP in figure 2(b). We also observe in figure 5(b) that the CTP excitation disappears when we consider a very narrow ring-like junction, an effect that can be explained as due to the fact that the conductance of a ring-like junction with $a_1 = 4\,\text{nm}$ and $a_2 = 5\,\text{nm}$ is $G = 224G_0$, below the conductance threshold for the emergence of the CTP, as derived from equation (5).

In figure 5(c) we represent the calculated normalized optical extinction cross-section for a nanoshell dimer linked by a conductive ring-like junction as the external radius a_2 is increased. In this case, the internal radius a_1 and the conductivity κ_J are fixed so that every spectrum is comparable to the spectrum of a solid junction with the same external radius. If we compare every ring-like junction spectrum to its solid junction counterpart, we observe that the modes remain in the same position and the main effect of removing the central part of the junction is an increase in the intensity of the resonance. Considering the results shown in figure 5(b), which suggest that conduction between the nanoparticles occurs mainly in the exterior of the junction, we expect the spectra for thick ring-like junctions to be very similar to their solid counterparts. A small hollow cavity with $a_1 = 0.5\,\text{nm}$ hardly affects the conduction process through the junction. This can be observed in figure 5(c), where the intensity of the BDP resonance decreases when the external radius is increased and the resonance is blue-shifted towards shorter

wavelength values, exactly as in the case of solid junctions (see figure 3). For the CTP resonance, its intensity is increased when the external radius is increased from 2.5 to 10 nm, and its peak position is blue-shifted, again consistent with the behaviour of a solid junction (see figure 3).

3. Excitonic junctions

Despite its simplicity, the pure conductor model for the junction is able to explain the main features of the optical response of linked plasmonic dimers. Now, we generalize the dielectric response of the linker by considering the existence of an optical interband transition in the response of the junction. The Lorentz model, widely used to study the optical properties of semiconductors, describes the interaction between light and atoms or molecules characterizing every entity through a resonant frequency ω_0 corresponding to the frequency of the molecular transition. We consider a linker composed of identical molecules with a single molecular transition of energy $\hbar\omega_0$ and characterized by the same geometric parameters as those used in the pure conductor model. According to the Drude–Lorentz model, the dielectric response function characterizing the junction can be expressed as [45]

$$\varepsilon(\omega) = 1 - \frac{f\omega_0^2}{(\omega^2 - \omega_0^2) + \mathrm{i}\omega\gamma}, \tag{8}$$

where ω_0 is the natural oscillator frequency of the molecular transition, γ is the transition damping and f describes the oscillator strength. This expression is quantitatively and qualitatively quite different from the expression provided by the previous model (see equation (1)), affecting the conduction properties. Now, both the real and imaginary parts of the conductivity $\kappa(\omega)$ contribute to the conduction process and they are also frequency dependent, in contrast to the pure conductor model. In order to establish a direct comparison with our previous model, the conductance G associated with this Drude–Lorentz model is related to the real part of the conductivity $\kappa_1(\omega) = \mathrm{Re}[\kappa(\omega)]$ as follows:

$$G = \kappa_1(\omega)\pi \left\{ \sqrt{R^2 - a^2} - R + (d/2 + R) \ln \left[1 + 2(R - \sqrt{R^2 - a^2}/d \right] \right\}, \tag{9}$$

where $\kappa_1(\omega)$ can be expressed in terms of $\varepsilon(\omega)$, according to equation (1). We also observe that the effect of increasing the size of the linker with the same transition wavelength is to increase the magnitude of the conductance, which presents resonant behaviour around the transition frequency ω_0.

In order to simplify the simulations, we have considered in this section a dimer of gold nanoparticles, instead of gold nanoshells, since the most relevant parameter is the external radius R. Thus, fixing their radius to $R = 50$ nm and the interparticle gap to $d = 1$ nm, the plasmon BDP resonance of the dimer is found at $\lambda_{\mathrm{BDP}} = 665$ nm. As a first step, we have considered two different molecules from the literature, a rotaxane and a J-aggregate [35, 38]. For the rotaxane, the transition frequency is $\omega_0 = 1.51$ eV, which corresponds to $\lambda_0 = 821$ nm, the damping factor is $\gamma = 0.1$ eV [38] and we have considered $f = 1.5$ as the oscillator strength factor. For the J-aggregate, the transition frequency is $\omega_0 = 1.79$ eV, which corresponds to $\lambda_0 = 693$ nm, the damping factor is $\gamma = 0.052$ eV and the oscillator strength factor is $f = 0.02$ [35].

Once the dielectric function is determined with these parameters, we vary the radius of the junction and explore the evolution of the normalized optical extinction cross-section in figure 6. For the rotaxane molecule (figure 6(a)) we observe that, as for the pure conductor,

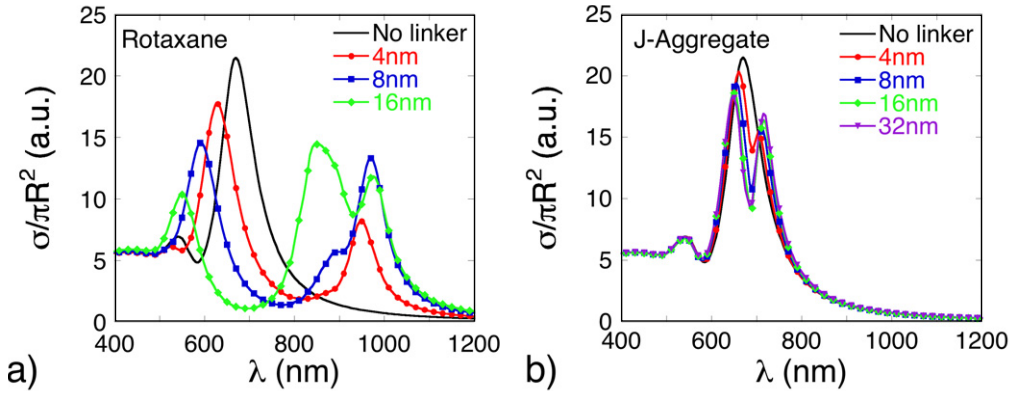

Figure 6. Calculated normalized optical extinction cross-section of a gold nanoparticle dimer bridged by a molecular linker as the radius of the linker a is increased. (a) Rotaxane molecule with molecular transition frequency $\omega_0 = 1.51\,\text{eV}$ ($\lambda_0 = 821\,\text{nm}$); (b) J-aggregate molecule with molecular transition frequency $\omega_0 = 1.79\,\text{eV}$ ($\lambda_0 = 693\,\text{nm}$).

the BDP mode, arising from the coupling between the dipolar modes of the individual particles and initially found at $\lambda = 665\,\text{nm}$, is blue-shifted as the radius of the linker is increased, progressively losing part of its intensity. This behaviour of the BDP mode is as expected, since the conditions are very similar to the situation depicted for the conductive junction in figure 3, where the conductivity of the junction is fixed, and the conductance is increased via an increase of the radius of the junction. Now, equation (9) shows that the increase of the radius of the molecular linker implies an increase of the conductance G as well. Nevertheless, the situation is different for longer wavelength values. For the pure conductor model, when the conductance is large enough a highly red-shifted CTP mode emerges, where a charge transfer between the particles occurs (see figure 3). However, in this generalized model, we observe in figure 6(a) the emergence of two red-shifted resonances as the radius of the linker becomes wider. From the near-field maps associated with the resonances, it can be checked that the most red-shifted resonance, around $\lambda \approx 1000\,\text{nm}$, also presents a BDP nature, exactly as the blue-shifted BDP. In contrast, the resonance in between, around $\lambda \approx 850\,\text{nm}$, presents a clear CTP nature, even though it is considerably less red-shifted than the CTP mode in the conductor model. It is clear from these results that the consideration of a more complex conductive nature characterizing the linker affects strongly the behaviour of the plasmonic cavity modes. We believe that this mix of the modes is a consequence of the coupling between the plasmon resonances of the cavity and the exciton introduced as an optical transition, a situation that could be exploited in new forms of sensing.

For the J-aggregate, in figure 6(b), the BDP mode also splits into two branches. In this case, the magnitude of the blue-shift is not as large as for the rotaxane. This can be explained as due to the low conductivity of the linker, several orders of magnitude below the conductivity of rotaxane and gold. We also observe that, for the J-aggregate, we do not appreciate the emergence of the CTP mode in between the two BDP coupled modes, even though we have dramatically increased the radius of the linker up to $a = 32\,\text{nm}$. Following the low conductivity argument, we know that the CTP mode needs really large conductance to be sustained, a condition that is not fulfilled by the extremely low conductivity of the molecule under consideration. A more

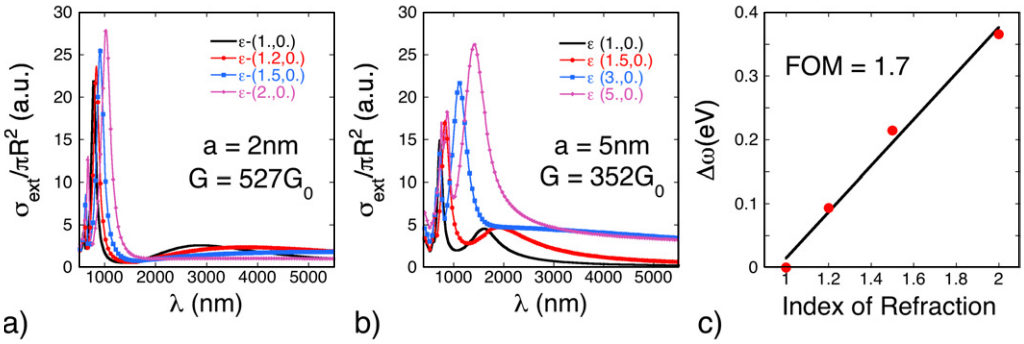

Figure 7. Sensitivity of the nanoparticle dimer to the embedding medium in the optical extinction spectra when (a) $a = 2\,\text{nm}$ and $G = 527G_0$ and (b) $a = 5\,\text{nm}$ and $G = 352G_0$. (c) Linear plot of the BDP shifts versus refractive index of the embedding medium for the junction parameters in (a).

exhaustive study of this coupling between the plasmon resonances and the excitons is currently in progress, but we can anticipate that large conductance values at NIR wavelengths are needed to noticeably modify the CTP.

4. Sensing with the use of bonding dimer plasmons and charge transfer plasmons

The potential use of plasmonic systems as sensors has led to many studies on their sensitivity to the embedding medium. We have also explored this sensitivity in the linked dimer system. In previous works, a redshift of the plasmon resonance was observed when the refractive index n of the surrounding medium is increased (thus increasing the real part of the dielectric function), in addition to an increase in its intensity [47, 48]. This behaviour was found to be systematic for different types of nanostructures, such as nanorods, nanoshells or nanodiscs; more recently, there has been growing interest in this kind of study using Fano resonances [49], because of the sharp spectral features.

Figure 7 shows the evolution of the normalized optical extinction cross-section of gold nanoshell dimers bridged by a conductive junction as the dielectric function of the embedding medium is varied. Two different linkers with high conductance have been considered: a junction with radius $a = 2\,\text{nm}$ and conductance $G = 527G_0$ in figure 7(a) and a junction with radius $a = 5\,\text{nm}$ and conductance $G = 352G_0$ in figure 7(b). In both cases, the BDP mode is redshifted and its intensity is increased when the dielectric constant of the surrounding medium is increased, as expected. In contrast, the CTP mode is just slightly redshifted before vanishing. Once more, the actual geometry of the cavity plays an important role: for wider junctions the CTP resonance survives for larger values of the dielectric function. Since narrower spectral peaks are more appropriate to measure small peak shifts, we focus our attention on the BDP mode to evaluate its sensitivity to the embedding medium.

The efficiency of plasmonic systems as sensors is usually estimated by its figure of merit (FOM). This parameter is defined as [48]

$$\text{FOM} = \frac{m\ (\text{eV RIU}^{-1})}{\text{fwhm (eV)}}, \tag{10}$$

where m is the linear regression slope for the refractive index dependence, which indicates the ratio of the plasmon energy shift to the change in refractive index of the embedding medium, and fwhm is the full-width at half-maximum of the mode. Figure 7(c) shows the linear plot of the shifts of the SBDP mode as a function of the refractive index of the embedding medium for $a = 2\,\text{nm}$ and $G = 527G_0$, where the slope given by the linear regression is $m = 0.36\,\text{eV RIU}^{-1}$. In this case, fwhm $= 0.21\,\text{eV}$ and the FOM parameter for the SBDP resonance is FOM $= 1.7$. For a junction with radius $a = 5\,\text{nm}$ and conductance $G = 352G_0$, $m = 0.21\,\text{eV RIU}^{-1}$ and fwhm $= 0.30\,\text{eV}$, resulting in an FOM $= 0.7$ parameter for the SBDP. These values indicate that the system with a narrower junction but higher conductance is more sensitive to the embedding medium. We can also consider the FOM parameter for the CTP mode, even though its broadening fwhm prevents large values. As an example, for the CTP mode in figure 7(b), we obtain $m = 0.22\,\text{eV RIU}^{-1}$ and fwhm $= 0.43\,\text{eV}$, resulting in an FOM parameter of FOM $= 0.5$, thus below the values for the BDP peaks.

5. Summary

We have studied theoretically how the optical properties of a nanoparticle dimer with a linker connecting two nanoparticles are affected by the size, conductivity and shape of the linker. We have started modelling the linker as a pure conductor with the shape of a cylinder, where conductivity is related to conductance through geometric parameters, and we have explored the behaviour of two optical resonances, the BDP and the CTP, sustained by the gap.

We have modelled the linker as a cylindrical shell to explore the spatial distribution of the conduction across the junction, observing that the electric current mainly takes place in the external part of the junction.

We have also analysed the effect of changes in the structure of the dielectric function characterizing the linker on the optical response by considering an optical transition at the linker. We have found that the coupling between the plasmon cavity modes and the excitons modifies the optical response considerably.

To complete this general picture, we have studied the sensitivity of the BDP and CTP plasmons to the surrounding medium as well. The dimers linked by narrower junctions are more sensitive to the embedding medium as the conductance increases, in comparison to dimers linked by wider junctions.

We believe that the study of this kind of structure will contribute to the development of plasmonic nanostructures as active devices, linking optical and transport properties.

Acknowledgments

This work was supported by the Etortek project inanoGUNE and the Etortek inano II project of the Basque Government (BG), project no. FIS2010-19609-C02-01 of the Spanish Ministry of Science and Innovation, grant no. IT-366-07 from BG-UPV/EHU and the project CUBIHOLE EUI2008-03816 of the European Union. Computational resources were provided by IZO-SGIker (UPV/EHU, MICINN, BG and ESF).

References

[1] Pelton M, Aizpurua J and Bryant G W 2008 *Laser Photon. Rev.* **2** 136–59
[2] Lal S, Link S and Halas N J 2008 *Nat. Photonics* **1** 641
[3] Aizpurua J, Hanarp P, Sutherland D S, Käll M, Bryant G W and García de Abajo F J 2003 *Phys. Rev. Lett.* **90** 057401
[4] Prodan E, Radloff C, Halas N J and Nordlander P 2003 *Science* **302** 419
[5] Link S and El-Sayed M A 1999 *J. Phys. Chem.* B **103** 8410
[6] Prescott S W and Mulvaney P J 2006 *J. Appl. Phys.* **99** 123504
[7] Aizpurua J, Bryant G W, Ritcher L J and García de Abajo F J 2005 *Phys. Rev.* B **71** 235420
[8] Hirsch L R, Gobin A M, Lowery A R, Tam F, Drezek R A, Halas N J and West J L 2006 *Ann. Biomed. Eng.* **34** 15
[9] Nordlander P, Oubre C, Prodan E, Li K and Stockman M I 2004 *Nano Lett.* **4** 899
[10] Kim D S, Heo J, Ahn S H, Han S W, Yun W S and Kim Z H 2009 *Nano Lett.* **9** 3619
[11] Yang S C, Kobori H, He C L, Lin M H, Chen H Y, Li C, Kanehara M, Teranishi T and Gwo S 2010 *Nano Lett.* **10** 632
[12] Xu H, Aizpurua J, Käll M and Apell P 2000 *Phys. Rev.* E **62** 4318
[13] Xu H, Bjerneld E J, Käll M and Börjesson L 1999 *Phys. Rev. Lett.* **83** 4357
[14] Ward D R, Halas N J, Ciszek J W, Tour J M, Wu Y, Nordlander P and Natelson D 2008 *Nano Lett.* **8** 919
[15] Zhang Z, Weber-Bargioni A, Wu S, Dhuey S, Cabrini S and Schuck P J 2009 *Nano Lett.* **9** 4505
[16] Atay T, Song J-H and Nurmikko A V 2004 *Nano Lett.* **4** 1627–31
[17] Romero I, Aizpurua J, García de Abajo F J and Bryant G W 2006 *Opt. Express* **14** 9988
[18] Danckwerts M and Novotny L 2007 *Phys. Rev. Lett.* **98** 026104
[19] Lassiter J B, Aizpurua J, Hernández L I, Brandl D W, Romero I, Lal S, Hafner J H, Nordlander P and Halas N J 2008 *Nano Lett.* **8** 1212
[20] Zuloaga J and Nordlander P 2009 *Nano Lett.* **9** 887–91
[21] Schnell M, García A Etxarri, Huber A, Aizpurua J and Hillenbrand R 2009 *Nat. Photonics* **3** 287
[22] van der Molen S J, Liao J, Kudernac T, Agustsson J S, Bernard L, Calame M, van Wees B J, Feringa B L and Schönenberger C 2009 *Nano Lett.* **9** 76–80
[23] Chau Y F, Lin Y-J and Tsai D P 2010 *Opt. Express* **18** 3510–18
[24] Park H, Park J, Lim A K L, Anderson E H, Alivisatos A P and McEuen P L 2000 *Nature* **407** 57–60
[25] Nazin G V, Qiu X H and Ho W 2003 *Science* **302** 77–81
[26] Dadosh T, Gordin Y, Krahne R, Khivrich I, Mahalu D, Frydman V, Sperling J, Yacoby A and Bar-Joseph I 2005 *Nature* **436** 677–80
[27] Venkataraman L, Klare J E, Tam I W, Nuckolls C, Hybertsen M S and Steigerwald M L 2006 *Nano Lett.* **6** 458–62
[28] Banerjee P, Conklin D, Nanayakkara S, Park T-H, Therien M J and Bonnell D A 2010 *ACS Nano* **4** 1019–25
[29] Liao J *et al* 2010 *Nano Lett.* **10** 759–64
[30] Reed M A, Zhou C, Muller C J, Burgin T P and Tour J M 1997 *Science* **278** 252–4
[31] Postma H W Ch, Teepen T, Yao Z, Grifoni M and Dekker C 2001 *Science* **293** 76–9
[32] Bachtold A, Hadley P, Nakanishi T and Dekker C 2001 *Science* **294** 1317–20
[33] Andrew P and Barnes W L 2004 *Science* **306** 1002
[34] Wurtz G A, Evans P R, Hendren W, Atkinson R, Dyckson W, Pollard R J and Zayats A V 2007 *Nano Lett.* **7** 1297
[35] Fofang N T, Park T, Neumann O, Mirin N A, Nordlander P and Halas N J 2008 *Nano Lett.* **8** 3481
[36] Hendry E, García-Vidal F J, Martín-Moreno L, Gómez-Rivas J, Bonn M, Hibbins A P and Lockyear M J 2008 *Phys. Rev. Lett.* **100** 123901
[37] Dintinger J, Klein S and Ebbesen T W 2006 *Adv. Mater.* **18** 1267
[38] Zheng Y B, Yang Y, Jensen L, Fang L, Juluri B K, Flood A H, Weiss P S, Stoddart J F and Huang T J 2009 *Nano Lett.* **9** 819

[39] Pérez-González O, Zabala N, Borisov A, Halas N J, Nordlander P and Aizpurua J 2010 *Nano Lett.* **10** 3090
[40] García de Abajo F J and Howie A 1998 *Phys. Rev. Lett.* **80** 5180
[41] García de Abajo F J and Howie A 2002 *Phys. Rev.* B **65** 115418
[42] Johnson P B and Christy R W 1972 *Phys. Rev.* B **6** 4370
[43] Palik E D 1985 *Handbook of Optical Constants* (New York: Academic)
[44] Fox M 2001 *Optical Properties of Solids* (New York: Oxford University Press)
[45] Dressel M and Grüner G 2002 *Electrodynamics of Solids* (Oxford: Cambridge University Press)
[46] Large N, Abb M, Aizpurua J and Muskens O L 2010 *Nano Lett.* **10** 1741
[47] Miller M and Lazarides A 2006 *J. Opt. A: Pure Appl. Opt.* **8** 239
[48] Sherry L J, Chang S H, Schatz G C and Van Duyne R P 2005 *Nano Lett.* **5** 2034
[49] Lassiter J B, Sobhani H, Fan J A, Kundu J, Capasso F, Nordlander P and Halas N J 2010 *Nano Lett.* **10** 3184